EPJ B
Condensed Matter and Complex Systems
www.epj.org

Eur. Phys. J. B **63**, 93–100 (2008) DOI: 10.1140/epjb/e2008-00212-0

Spontaneous-search method and short-time dynamics: applications to the Domany-Kinzel cellular automaton

S.D. da Cunha, U.L. Fulco, L.R. da Silva and F.D. Nobre

EDP SCIENCES
Società Italiana di Fisica
Springer

Eur. Phys. J. B **63**, 93–100 (2008)
DOI: 10.1140/epjb/e2008-00212-0

THE EUROPEAN PHYSICAL JOURNAL B

Spontaneous-search method and short-time dynamics: applications to the Domany-Kinzel cellular automaton

S.D. da Cunha[1], U.L. Fulco[2], L.R. da Silva[1], and F.D. Nobre[3,a]

[1] Departamento de Física Teórica e Experimental, Universidade Federal do Rio Grande do Norte, Campus Universitário – C.P. 1641, 59072-970 Natal – RN, Brazil
[2] Departamento de Biofísica e Farmacologia, Universidade Federal do Rio Grande do Norte, Campus Universitário – Lagoa Nova, 59078-972 Natal – RN, Brazil
[3] Centro Brasileiro de Pesquisas Físicas, Rua Xavier Sigaud 150, 22290-180 Rio de Janeiro – RJ, Brazil

Received 3 May 2007 / Received in final form 1st April 2008
Published online 6 June 2008 –

Abstract. The one-dimensional Domany-Kinzel cellular automaton is investigated by two numerical approaches: (i) the spontaneous-search method, which is a method appropriated for a search of criticality; (ii) short-time dynamics. Both critical frontiers of the system are investigated, namely, the one separating the frozen and active phases, as well as the critical line determined by damage spreading between two cellular automata, that splits the active phase into the nonchaotic and chaotic phases. The efficiency of the spontaneous-search method is established herein through a precise estimate of both critical frontiers, and in addition to that, it is shown that this method may also be used in the determination of the critical exponent $\nu_\perp$. Using the critical frontiers obtained, other exponents are estimated through short-time dynamics. It is verified that the critical exponents of both critical frontiers fall in the universality class of directed percolation.

PACS. 05.70.Ln Nonequilibrium and irreversible thermodynamics – 64.60.Ht Dynamic critical phenomena – 64.60.-i General studies of phase transitions

1 Introduction

Cellular automata are dynamical systems with applications in many areas of science, like physics, chemistry, biology, and computation [1]. They are very convenient from the computational point of view, since they are defined in terms of a discrete-time evolution of a given set of variables (essentially, discrete variables) in a lattice (i.e., discrete space). In most cases, all variables are updated at once (i.e., parallel dynamics) through dynamical rules, that may be either probabilistic or deterministic, defined in such a way that in each time step, the new variables depend on the states of their neighboring variables at the previous time. Since the updating rules do not follow necessarily a Boltzmann weight or a detailed-balance condition, the system does not reach a standard equilibrium state, and for this reason, it may be appropriate for describing out-of-equilibrium situations, like crystal growth, turbulence, and chemical reactions.

Contrary to what happens in equilibrium models, which after some time of a numerical simulation (usually known as the "equilibration time") reach a state that does not exhibit interesting dynamical effects, nonequilibrium models, like cellular automata, may present curious behavior, e.g., nonequilibrium phase transitions [2,3]. In this case, time plays an important role, and is usually considered as an additional dimension. Since time and space present different characteristics, one needs to distinguish the physical properties in these two dimensions, in such a way that one frequently associates to them the indices $\parallel$ and $\perp$, respectively. The corresponding phase transitions are characterized by two independent correlation lengths, namely, a temporal length scale $\xi_\parallel$, and a spatial length scale $\xi_\perp$, which should both diverge at criticality, with different exponents, $\nu_\parallel$ and $\nu_\perp$, respectively.

Among many cellular automata studied in the literature [1–3], the one-dimensional (as usual, this nomenclature applies to the spatial dimension only) Domany-Kinzel cellular automaton (DKCA) [4,5] appears as one of the most investigated. This great interest comes from the fact that it is a simple probabilistic cellular automaton exhibiting phase transitions. The DKCA presents a critical frontier separating an active from an inactive (frozen) phase; in the former, a fluctuating steady state exists, whereas in the latter, the system always attains the absorbing state, characterized by a configuration that the system can reach, but cannot escape. This is the only phase transition that appears in the DKCA if one gets restricted to

[a] e-mail: fdnobre@cbpf.br

an analysis of a single copy of the automaton. However, the DKCA has been investigated also within the damage-spreading technique, which consists in following the time evolution of two configurations that differ, at an initial time, in the states of some of its variables (commonly denominated of an initial "damage") [6]. In this case, one finds that the active phase of the DKCA splits into two new phases, namely, the chaotic (where the initial damage tends to increase in time) and the nonchaotic (where the initial damage is suppressed after some time) ones.

The directed percolation (DP) problem provides a universality class that covers a wide range of models, which have in common the existence of an absorbing state [2,3]. The remarkable aspect of DP concerns its robustness with respect to the microscopic dynamic rules involved, leading to a conjecture [7,8] that, any model presenting a continuous phase transition from a fluctuating active phase to a unique absorbing state, characterized by a positive one-component order parameter, following a dynamics defined in terms local (i.e., short-range) rules, should fall in the DP universality class. It is well-accepted nowadays that the critical frontier frozen-active of the DKCA falls in the DP universality class, except for a single terminal point, which is known to belong the the compact DP class [4,9,10]. Apart from that, there is numerical evidence that the critical frontier nonchaotic-chaotic should also belong to the DP universality class [11].

The spontaneous-search method (SSM) is inspired on the concept of self-organized criticality [12], according to which certain dynamical systems evolve spontaneously towards the critical state, i.e., the critical state is an attractor of the dynamics. A conceptual framework for such phenomena was proposed in reference [13], based on the idea that a control rule, designed to keep the order parameter close to a small positive value, pushes the system automatically to the vicinity of the critical point. The SSM is based on a recursive relation, in such a way to implement operationally the proposal of reference [13]. By an appropriate choice of the order parameter, the recursion drives certain physical systems spontaneously to the value of the control parameter associated with such a choice; in particular, if the order parameter is set to a small value, the system will be driven towards the critical point. The SSM was introduced for the determination of critical properties in polymers [14] and percolation [15]; later on, it was successfully applied to magnetic systems [16–18]. This method uses an algorithm based on a recursive relation,

$$X_{n+1} = X_n - \alpha\ (Y_n - Y^*), \tag{1}$$

involving two dimensionless variables (X_n, Y_n), associated with the parameters of a given physical system. The variables (X_n, Y_n) change at each iteration step n, in such a way that after a sufficient number of steps, X_n will converge to a stationary value X^*, compatible with the stationary value $Y^* \equiv Y(X^*)$, assumed by Y_n. The desired stationary state (X^*, Y^*) may be previously chosen by setting the input quantity Y^*; at the first iteration, one chooses the initial value X_0, which will define the range of parameters to be investigated [(X_n, Y_n) will vary from (X_0, Y_0) to (X^*, Y^*)], whereas the rate of convergence to the stationary state is controlled by the parameter α. As an example, for a simple ferromagnet, such quantities may be related to the temperature and magnetization, respectively [16–18]; instead of performing a careful sweep in the temperature T, one may reach criticality by taking the magnetization $m \to 0^+$, which is equivalent to approaching the critical temperature, $T \to T_c^-$.

Numerical simulations in the short-time regime, commonly known as short-time-dynamics (STD) simulations, became an important tool in the investigation of critical phenomena [19], based on the curious aspect that important scaling behavior seems to be already present in the early stages of the dynamical evolution of some statistical-mechanics models, at criticality [20]. A significant reduction in the computational effort comes out from the STD approach, when compared with standard numerical simulations, essentially due to the following aspects: (i) the smaller times that one is concerned in STD; (ii) at its early stage of evolution the system presents small spatial and temporal correlation lengths, leading to a substantial reduction of finite-size effects. Since in the STD simulations one is dealing with an out-of-equilibrium regime, the scaling behaviors should depend on the initial conditions, in such a way that several scaling forms, associated essentially with different initial conditions for the moments of the order parameter, have been proposed and verified numerically in the literature (see, e.g., Refs. [19,21–24]). As a simple illustration, one may consider a ferromagnetic Ising model, described in terms of binary variables, $S_i(t) = \pm 1$, for which one may represent the k-th moment of the magnetization at time t, as

$$M^{(k)}(t) = \frac{1}{N^k} \left\langle \left(\sum_{i=1}^{N} S_i(t) \right)^k \right\rangle, \tag{2}$$

where N stands for the total number of spins of the lattice, and $\langle .. \rangle$ represents an average over different samples at time t, i.e., an average over distinct sequences of random numbers up to time t. For this system, different initial conditions are essentially taken into account through the definition of the initial magnetization of the system. If the system is quenched from an initial state with a small magnetization, $M(0) \ll 1$, one gets for the magnetization at time t [herein we use the standard notation, $M^{(1)}(t) \equiv M(t)$] and its second moment, respectively,

$$M(t) \sim M(0) t^{\theta}, \tag{3}$$

$$M^{(2)}(t) \sim t^{(d-2\beta/\nu)/z}, \tag{4}$$

where d corresponds to the lattice dimension. In the scaling laws above, the standard equilibrium exponents β and ν (which corresponds to $\nu_\perp$ in the DKCA), as well as the dynamic exponent z, appear, leading to the possibility of evaluating them already for very short times of the evolution of the system. However, a new and independent dynamical exponent arises, θ, which is related to the increase of the magnetization at the critical temperature, when the

system is quenched from a high-temperature state. In order to compute θ from equation (3) one should consider distinct, small (although finite) values of $M(0)$, and then take an extrapolation to $M(0) \to 0$. An equivalent way to carry on such a procedure consists in starting with a random initial configuration (i.e., magnetization and correlation length both equal to zero) and computing the correlation function [23],

$$Q(t) = \frac{1}{N} \left\langle \sum_{i,j=1}^{N} S_i(t) S_j(0) \right\rangle \sim t^{\theta}. \tag{5}$$

Now, if one starts the system with a completely ordered configuration [$M(0) = 1$], the magnetization should follow the simple power-law behavior,

$$M(t) \sim t^{-\beta/(\nu z)}. \tag{6}$$

For such an Ising model, one may also define quantities that take into account mixed initial conditions, like [24]

$$F_2(t) = \frac{M^{(2)}(t, L)|_{M(0)=0}}{[M(t, L)]^2|_{M(0)=1}} \sim t^{d/z}. \tag{7}$$

Apart from the scalings above, other forms have been proposed, involving higher-order moments of the order parameters in both initial conditions (i.e., completely random and ordered initial configurations), in such a way that it is possible to find all the exponents defined above through STD simulations.

In the present work we investigate the one-dimensional DKCA. Considering a single copy of the DKCA we analyze the critical frontier frozen-active; following the time evolution of two copies of the DKCA we study the critical frontier nonchaotic-chaotic that splits the active phase. In both cases, we use the spontaneous-search method, which appears to be very accurate for the determination of the critical frontiers, and we show how this technique may be used also to estimate the critical exponent $\nu_{\perp}$; the effectiveness of the method is verified herein for the DKCA. Using the critical frontiers determined through the spontaneous-search method, we apply short-time dynamics to obtain other critical exponents. Our critical-exponent estimates indicate that both critical frontiers of the DKCA fall in the DP universality class. In the next section we define the numerical procedures to be used; in Section 3 we present and discuss our results.

2 The model and numerical procedure

Let us consider the one-dimensional DKCA, consisting of a linear chain of L sites, with periodic boundary conditions; all sites are occupied by binary variables, in such a way that at each instant of time t, $\sigma_i(t) = 0, 1$ ($i = 1, 2, ..., L$). The state of the system at a given time t is specified by the set of all variables, $\{\sigma_i(t)\}$. The one-dimensional DKCA is usually defined in its symmetric form, in terms of the conditional probabilities, $\{P[\sigma_{i-1}(t), \sigma_{i+1}(t)|\sigma_i(t+1)]\}$, for the state of site i at time $t+1$, depending on the states of the variables at its nearest-neighboring sites, at the previous time. However, for computational purposes, it is more convenient to work with the DKCA in its nonsymmetric form [6,25,26], for which the conditional probability associated with the state of the variable $\{\sigma_i(t+1)\}$ depends on the previous states of the variable itself, as well as of one of its neighboring sites, e.g., $\{P[\sigma_i(t), \sigma_{i+1}(t)|\sigma_i(t+1)]\}$. Herein, we shall work with this later formulation, with the conditional probabilities given by $P(0,1|1) = P(1,0|1) = p_1$, $P(1,1|1) = p_2$, $P(0,0|1) = 0$; obviously, $P[\sigma_i(t), \sigma_{i+1}(t)|0] = 1 - P[\sigma_i(t), \sigma_{i+1}(t)|1]$. In order to describe the possible phase transitions of the DKCA, let us define the average density of active sites,

$$\rho(t) = \left\langle \frac{1}{L} \sum_{i=1}^{L} \sigma_i(t) \right\rangle, \tag{8}$$

which is defined for a single copy of the DKCA. Another important parameter in this problem [6] consists in the average Hamming distance between two copies A and B of the DKCA,

$$\psi(t) = \left\langle \frac{1}{L} \sum_{i=1}^{L} |\sigma_i^A(t) - \sigma_i^B(t)| \right\rangle. \tag{9}$$

In the equations above, $\langle ..\rangle$ denotes an average over independent realizations, i.e., an average over different initial states of the DKCA. It is important to remind that, in principle, there are two limits to be performed in the present problem, namely, $t \to \infty$ and $L \to \infty$, although within the STD approach, only the thermodynamic limit will be considered. As will be discussed in detail further on, the results of the SSM depend on the relaxation time (to be called hereafter $t_{\rm rel}$) of the automaton. After relaxation, we apply the SSM for a given finite time interval, over which one gets a convergence on the respective recursive relations; once this convergence is attained, the results of the SSM do not change, within the error bars, by considering this method over larger time intervals. For each given value of L, we extrapolate the results of the SSM to the limit $t_{\rm rel} \to \infty$ and whenever the limits $t_{\rm rel} \to \infty$ and $L \to \infty$ become necessary, we will assume that they may be freely interchanged; in the present analysis we will be restricted to the order $t_{\rm rel} \to \infty$ first, and then, $L \to \infty$. Considering these extrapolations, the quantities in equations (8) and (9) represent the order parameters of the DKCA. For a given finite time, after the automaton relaxation, the phase transition separating the frozen and active phases is signaled by the onset of the stationary value of the average density of active sites of equation (8), whereas the phase transition that splits the active phase into the nonchaotic and chaotic phases can be detected only by considering two copies (A and B) of the system, through the stationary value of the average Hamming distance defined in equation (9).

In order to implement the SSM for the determination of the critical frontiers of the DKCA, we will make use of recursive relations, like the one of equation (1). Before

doing that, we let the automaton relax for a given time $t_{\rm rel}$; then, we choose one of the probabilities (p_1 or p_2) to keep fixed, and apply the respective recursive relation in the search for the critical value associated with the remaining probability; this corresponds to the initial time ($t = 0$) for the SSM. For the critical frontier frozen-active, we fix p_2 to a given value in the range [0,1] and analyze the convergence of $p_1(L,t)$ to the associated value at the critical frontier, according to

$$p_1(L,t+1) = p_1(L,t) - b[\rho(t) - (1/L)]. \qquad (10)$$

For the critical frontier nonchaotic-chaotic, we have chosen to set p_1 to a high value, presumably in the region where the desired frontier is present, and follow the time evolution of $p_2(L,t)$,

$$p_2(L,t+1) = p_2(L,t) + c[\psi(t) - (1/L)]. \qquad (11)$$

In the equations above, the constants b and c are set to small positive values, and their magnitude control the rate of convergence to the critical frontier; once the critical frontier is approached, fluctuations $O(1/L)$ occur around the desired critical point. The different signs preceding constants b and c in equations (10) and (11) tend to produce a small positive (negative) increment in the investigated probability, if one is below (above) the critical point.

The convergence of the SSM occurs for relatively small times (essentially for $t \approx 100$ steps), although we have verified a strong dependence of this procedure in $t_{\rm rel}$, in the sense that for each relaxation time $t_{\rm rel}$, one gets a different convergence in the corresponding recursion relation. Therefore an extrapolation $t_{\rm rel} \to \infty$ is necessary in order to obtain the average stationary probability, $\bar{p_1}(L)$ [or $\bar{p_2}(L)$], which depends now only on the size L. By analyzing different sizes, one may extrapolate these probabilities to the thermodynamic limit; in addition to that, one can also compute the critical exponent $\nu_\perp$, associated with the corresponding critical frontier, by using the scaling relations,

$$\bar{p_1}(L) - p_{1c} \sim L^{-1/\nu_\perp}, \qquad \text{and} \qquad \bar{p_2}(L) - p_{2c} \sim L^{-1/\nu'_\perp}. \qquad (12)$$

In the equations above, p_{1c} and p_{2c} represent the extrapolated critical probabilities, in the thermodynamic limit, associated with the critical frontiers calculated from the set of data $\{\bar{p_1}(L)\}$ [obtained from Eq. (10)] and $\{\bar{p_2}(L)\}$ [obtained from Eq. (11)], respectively. Furthermore, $\nu_\perp$ and $\nu'_\perp$ represent their respective critical exponents.

The STD approach consists in numerical simulations carried at criticality, for a short time t greater than a certain microscopic time scale. This method has been applied successfully in a wide variety of magnetic systems [19], for which several interesting power-law behaviors were observed at short times, and it was used also for the investigation of the critical behavior of nonequilibrium models (cf., e.g., Ref. [27]). As mentioned in the previous section, due to its short-time character, the scaling behaviors should depend on the initial conditions; herein, we will consider such conditions directly associated with the order parameters of the DKCA at initial times, $t = 0$. Herein, we suppose that the STD technique leads to scaling relations for the order parameters of the DKCA similar to those of the ferromagnetic Ising model, presented in the previous section; such an assumption will be confirmed in the next section. It should be mentioned that, although considered in two different numerical procedures, the variable t considered in the STD approach corresponds to the same time variable used in the SSM [cf. Eqs. (10) and (11)], i.e., in both cases each unit of time corresponds to a simultaneous updating of all variables $\{\sigma_i(t)\}$.

Therefore, considering small initial values [$O(1/L)$] for the order parameters, one should have [cf. Eq. (3)]

$$\rho(t) \sim t^{\theta}; \qquad \psi(t) \sim t^{\theta'}, \qquad (13)$$

whereas if one starts the system with the order parameters at their maximum values, then [cf. Eq. (6)]

$$\rho(t) \sim t^{-\beta/\nu_\parallel}; \qquad \psi(t) \sim t^{-\beta'/\nu'_\parallel}, \qquad (14)$$

where the primed exponents apply to the critical frontier nonchaotic-chaotic and we have used that $z = \nu_\parallel/\nu_\perp$. The validity of these power-law behaviors for the DKCA, at short times, will be verified in the next section. From the exponents of equations (13) and (14) one may estimate the dynamical exponent z by using the scaling relation,

$$\theta + 2\,\frac{\beta}{\nu_\parallel} = d\frac{\nu_\perp}{\nu_\parallel} \qquad \Rightarrow \qquad \theta + 2\frac{\beta}{\nu_\parallel} = \frac{d}{z}, \qquad (15)$$

where d denotes the space dimension ($d = 1$ in the present problem); similar relations hold for the primed exponents. Based on these relations, authors have calculated the dynamic exponent z directly by computing the ratio between one of the quantities in equation (13) and the square of the analogous quantity in equation (14) [27].

In the next section we present and discuss the results obtained by applying the SSM and STD to investigate the critical properties of the DKCA.

3 Results and discussion

The DKCA was studied in its nonsymmetric form, as defined above. If not specified explicitly, all realizations started with random initial configurations, by assigning to each site an equal probability for its variable to be in one of the two possible states.

In the application of the SSM for the frontier frozen-active, before using the appropriate recursive relation, we let the system relax for a given time, $t_{\rm rel}$. For the critical frontier nonchaotic-chaotic, the replica A was generated randomly, and it was let to evolve for a time $\Delta t = 5000$; at this time, a copy of it was made (copy B), at which the initial damage was introduced, by changing some of its variables $\{\sigma_i^B(t)\}$. Then, both copies were let to evolve towards relaxation (time $t_{\rm rel}$), and after that, the corresponding recursive relation of the SSM was applied. It is important to stress that, as usual, the same sequences of random numbers were used for copies A and B, in order to

ensure that the possible differences between these copies, at later times, should be due only to the initial damage. Larger times for the first evolution process of copy A (e.g., $\Delta t = 20\,000$) did not change our results, within the error bars. Different relaxation times were used (constructed from successive multiplications by factors of 2), $t_{\rm rel} = 1600, 3200, \ldots, 102\,400$, for the time extrapolations $t_{\rm rel} \to \infty$. These procedures were considered for each of the linear sizes, $L = 2500, 3750, 5000, 7500,$ and $10\,000$, from which the thermodynamic limit was considered. Samples averages were carried over $N_s = 3000$ independent realizations. For the constants b and c, in equations (10) and (11) respectively, we have used typically, $b = c = 0.005$ close to criticality, although slightly larger values for these constants were employed far from criticality, for quicker convergences of the SSM. For large values of L, the particular choices of the constants b and c are essentially related to the rate of convergence to criticality, e.g., larger values for these quantities lead to a faster convergence of the SSM. However, for small values of L, greater values for b and c also lead to larger fluctuations around the critical point. Neverthless, we have verified that, for sufficiently large values of L, the results of the SSM are independent of these choices.

It is important to mention that there are two possible variants of the DKCA [11], in what concerns the use of random numbers in the updating rules of the variables of the automaton, following the conditional probabilities $P(0,1|1) = P(1,0|1) = p_1$ and $P(1,1|1) = p_2$, as defined above. One may use either (i) different, or (ii) the same random numbers when dealing with probabilities p_1 and p_2. The critical frontiers happen to be a little different in these two cases, and specially the chaotic phase turns out to be slightly larger in case (i). We have verified that the SSM yields precise estimates of the critical frontiers for both variants of the DKCA, and below we shall present the results obtained by using variant (ii).

In Figure 1 we exhibit the time evolution ruled by equation (11), for a DKCA of linear size $L = 10\,000$, in the search for a point of the critical frontier nonchaotic-chaotic associated to the fixed value $p_1 = 0.95$. The time $t = 0$ in Figure 1a corresponds to the initial time for the SSM, after the relaxation process over $t_{\rm rel}$ steps, as described above. One observes that the recursive relation drives the system quickly to a basin of attraction, with the probability $p_2(L,t)$ presenting small fluctuations around a given average value. However, the stationary value of $p_2(L,t)$ depends strongly on the relaxation time used, although for a given relaxation time, the stationary value obtained is essentially independent of the initial condition $p_2(L,0)$ used for the SSM (see, e.g., two very distinct initial conditions, namely, $p_2(L,0) = 0$ and $p_2(L,0) = 1$, used for the relaxation times $t_{\rm rel} = 3200$ and $25\,600$). As expected, the difference between the stationary values associated with two successive relaxation times decreases for increasing values of the relaxation time, indicating a convergence for large values of $t_{\rm rel}$. For each relaxation time considered, one may use the last 500 time steps of the SSM in order to get a statistics, i.e., the average value and corresponding error bars for the stationary probability. After that, one may estimate the average probability $\bar{p_2}(L)$, associated with a given size L, by considering an extrapolation of the data obtained for distinct values of $t_{\rm rel}$, to the limit $t_{\rm rel} \to \infty$, as illustrated in Figure 1b.

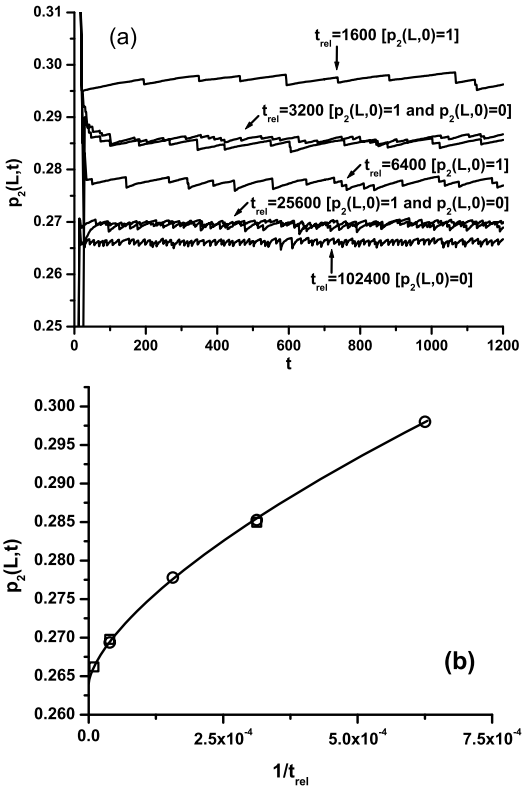

Fig. 1. (a) The probability $p_2(L,t)$ calculated from the SSM [Eq. (11)] for $p_1 = 0.95$ and different relaxation times. Herein, $t = 0$ corresponds to the initial time for the SSM, set right after the relaxation process over $t_{\rm rel}$ time steps. The linear size considered was $L = 10\,000$. (b) Plot of $p_2(L,t)$ versus $1/t_{\rm rel}$ showing the extrapolation to the limit $t_{\rm rel} \to \infty$ of the data in (a), leading to the extrapolated value $\bar{p_2}(L) = 0.26386$. The error bars are typically of the size of the symbols and squares (circles) correspond to the initial condition $p_2(L,0) = 0$ $[p_2(L,0) = 1]$.

Applying the same procedure described above for the critical frontier frozen-active, one may obtain a set of probabilities, $\{\bar{p_1}(L)\}$, which depend only on the size L. In Figure 2 we exhibit a nonlinear fit, according to the behavior presented in equation (12), for the point of this critical frontier corresponding to $p_2 = 0.5$. The error bars presented were obtained from the extrapolations $t_{\rm rel} \to \infty$, for each size L. By using the probabilities $\{\bar{p_1}(L)\}$, associated with five different sizes, namely, $L = 2500, 3750, 5000, 7500,$ and $10\,000$, our fit yielded $p_{1c} = 0.7493 \pm 0.0003$ and $\nu_\perp = 1.099 \pm 0.015$. The inset shows a plot of $\ln[p_{1c} - \bar{p_1}(L)]$ versus $\ln(1/L)$, using this value of p_{1c} obtained from the nonlinear fit; the slope of the straight line yields an estimate for $1/\nu_\perp$ that is in agreement with the value of $\nu_\perp$ obtained from the nonlinear fit, within the error bars. We have analyzed

Table 1. Coordinates of typical points of the critical frontier frozen-active of the nonsymmetric DKCA within variant (ii) [which corresponds to the use of the same random numbers when dealing with probabilities p_1 and p_2 (see text)], as obtained from the SSM, are compared to other results available in the literature.

p_2	1.00	0.80	0.50	0.20	0.00
p_{1c}	0.5000 ± 0.0002	0.6762 ± 0.0001	0.7493 ± 0.0003	0.7893 ± 0.0001	0.8095 ± 0.0003
Other estimates	1/2 (Ref. [28])	–	0.749 ± 0.001 (Ref. [26])	–	0.8095 (Ref. [26])

Table 2. Coordinates of typical points of the critical frontier nonchaotic-chaotic of the nonsymmetric DKCA within variant (ii) which corresponds to the use of the same random numbers when dealing with probabilities p_1 and p_2 (see text), as obtained from the SSM, are compared to other results available in the literature.

p_1	1.00	0.95	0.90	0.85
p_{2c}	0.3119 ± 0.0002	0.2641 ± 0.0003	0.2092 ± 0.0001	0.1390 ± 0.0003
Other estimates	0.31215 ± 0.00004 (Ref. [11])	–	–	0.1400 ± 0.0002 (Ref. [11])

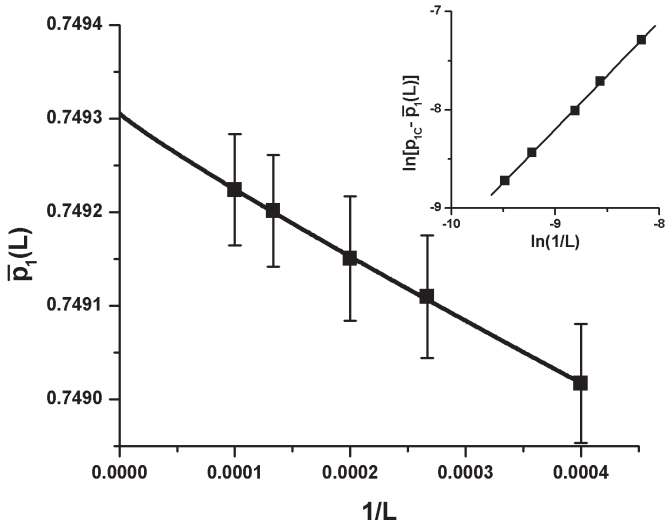

Fig. 2. Nonlinear fit (full line) of the probabilities $\{\bar{p_1}(L)\}$ versus $1/L$, for five different sizes of the system, corresponding to the point of the critical frontier frozen-active with $p_2 = 0.5$. In the inset we show a log-log (base e) plot using the critical value p_{1c} obtained from the extrapolation $L \to \infty$ of the nonlinear fit; the slope of the straight line yields an estimate for $1/\nu_\perp$, in agreement with the one obtained from the nonlinear fit.

other points along the critical frontier frozen-active and some of our estimates for p_{1c} are presented in Table 1. It should be pointed out that such estimates are in agreement (within the error bars), with other estimates available in the literature, obtained from the application of different approaches to the nonsymmetric DKCA, e.g., references [26,28]. In what concerns the critical-exponent $\nu_\perp$, the estimate above falls in the DP universality class (within the error bars), for which $\nu_\perp = 1.096854(4)$ [29]. Except for the terminal point $p_2 = 1$, which is well-known to lie in a different universality class, i.e., the class of compact DP, all points considered in the critical frontier frozen-active yielded estimates for $\nu_\perp$ in the DP universality class.

We have also applied nonlinear fits similar to the one of Figure 2 to sets of probabilities $\{\bar{p_2}(L)\}$, corresponding to

Table 3. The critical exponents for both critical frontiers of the DKCA. The estimates of $\nu_\perp$ and $\nu'_\perp$ follow from the SSM (see text); other exponents were computed from the STD technique, as well as through scaling relations. For comparison, estimates of the DP problem are included.

Critical Exponent	Frontier Frozen-Active	Frontier Nonchaotic-Chaotic	DP Ref. [29]
$\nu_\perp$, $\nu'_\perp$	1.099 ± 0.015	1.094 ± 0.014	1.096854(4)
θ, θ'	0.308 ± 0.005	0.316 ± 0.004	0.313686(8)
z, z'	1.618 ± 0.039	1.602 ± 0.041	1.580745(10)
$\nu_\parallel$, $\nu'_\parallel$	1.778 ± 0.052	1.752 ± 0.037	1.733847(6)
β, β'	0.276 ± 0.009	0.270 ± 0.011	0.276486(8)

different points along the nonchaotic-chaotic critical frontier. The critical points obtained are in good agreement with those available in the literature, and some of them are presented in Table 2. For the critical exponent $\nu'_\perp$, two different critical points, corresponding to $p_1 = 1$ and $p_1 = 0.95$, yielded the estimates, $(\nu'_\perp)^{-1} = 0.916 \pm 0.011$ and $(\nu'_\perp)^{-1} = 0.913 \pm 0.012$, respectively. Considering the average of these two estimates, one gets that $\nu'_\perp = 1.094 \pm 0.014$ (cf. Table 3). The phase diagram resulting from the application of the SSM to both critical frontiers of the nonsymmetric DKCA in its variant (ii) described above, using equation (10) (critical frontier frozen-active) and equation (11) (critical frontier nonchaotic-chaotic), is presented in Figure 3.

After a precise determination of the critical frontiers, as well as of the corresponding exponents $\nu_\perp$ and $\nu'_\perp$ from the SSM, one may use now other approximative methods for the estimation of different critical exponents. Herein, we make use of the STD technique [19], which was applied for the DKCA only recently, in an investigation of the critical frontier frozen-active [27]. Contrary to what was done in the SSM, the STD simulations do not follow the relaxation process characterized by the time $t_{\rm rel}$, i.e., $t_{\rm rel} = 0$. Therefore, in what concerns the critical frontier frozen-active, the time $t = 0$ corresponds to time right after the generation of the initial configuration. However, in the case of the critical frontier nonchaotic-chaotic, we also let copy A evolve initially for a time $\Delta t = 5000$, in order to attain its stationary state, before creating copy B (we have used higher values for Δt as well, and our

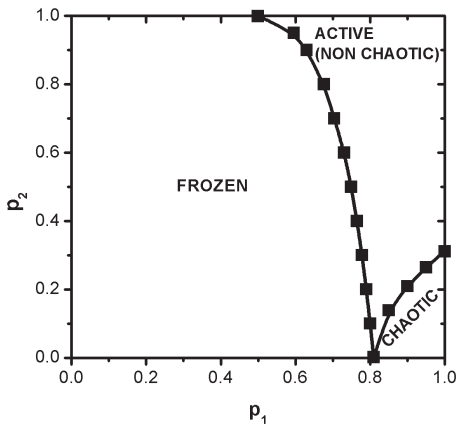

Fig. 3. Phase diagram of the nonsymmetric DKCA obtained from the SSM. The squares represent points obtained from the SSM; the full lines are guides to the eye.

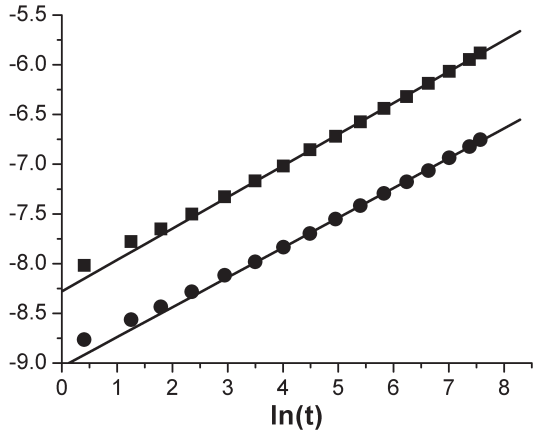

Fig. 4. Log-log (base e) plots of the order parameters of the DKCA, at criticality, versus time, within the STD approach. The order parameters $\rho(t)$ (circles) and $\Psi(t)$ (squares) are associated with the critical frontiers frozen-active and nonchaotic-chaotic, respectively. In both cases the initial order parameters (at time $t = 0$) were considered with infinitesimal values. The slopes of the straight lines yield the exponents θ and θ' [cf. Eq. (13)].

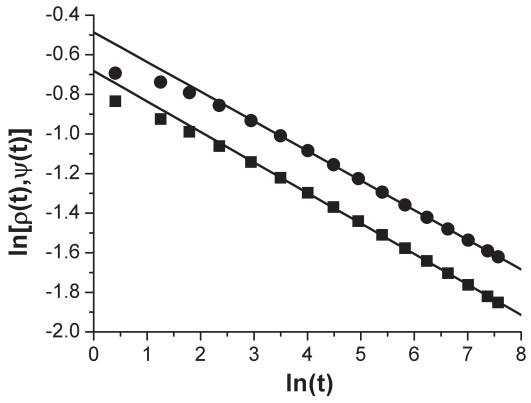

Fig. 5. Log-log (base e) plots of the order parameters of the DKCA, at criticality, versus time, within the STD approach. The order parameters $\rho(t)$ (circles) and $\Psi(t)$ (squares) are associated with the critical frontiers frozen-active and nonchaotic-chaotic, respectively. In both cases the initial order parameters (at time $t = 0$) were considered with their maximum values. The slopes of the straight lines yield the ratios of exponents, $-\beta/\nu_\parallel$ and $-\beta'/\nu'_\parallel$ [cf. Eq. (14)].

results did not change within the error bars); then, we create copy B, introduce the initial damage, and set the time $t = 0$ for the STD method. Using the procedures described in the previous section [cf. Eqs. (13) and (14)], we may obtain estimates for the exponents θ and the ratio $\beta/\nu_\parallel$, associated with the critical frontier frozen-active (the same applies to its counterparts, θ' and $\beta'/\nu'_\parallel$, of the critical frontier nonchaotic-chaotic). In Figures 4 and 5 we exhibit log-log plots of the order parameters of the DKCA, at criticality, versus time, obtained from the STD approach. The data presented correspond to a linear size $L = 10\,000$, to a maximum time of 2000 time steps, and to sample averages over $N_s = 10\,000$ independent realizations. The data for the order parameter $\rho(t)$ (circles) correspond to the point of the critical frontier frozen-active with $p_2 = 0.5$ (see Tab. 1), whereas those associated to $\Psi(t)$ (squares) correspond to the point $p_1 = 1.0$ of the critical frontier nonchaotic-chaotic (see Tab. 2). In Figure 4 the slopes of the straight lines yield $\theta = 0.308 \pm 0.005$ and $\theta' = 0.316 \pm 0.004$, respectively. From Figure 5 one gets that $\beta/\nu_\parallel = 0.155 \pm 0.005$ and $\beta'/\nu'_\parallel = 0.154 \pm 0.006$. Then, using the scaling relation of equation (15), one may estimate the dynamic exponent z, which, together with the estimate of $\nu_\perp$ obtained from the SSM, yields $\nu_\parallel$. All other exponents may be calculated from these estimates, using scaling relations (see Tab. 3). A similar procedure applies to the primed exponents, associated with the critical frontier nonchaotic-chaotic. The STD technique, applied recently for evaluating the critical exponents z and $\nu_\parallel$ of the critical frontier frozen-active of the DKCA, yielded $z = 1.581 \pm 0.001$ and $\nu_\parallel = 1.731 \pm 0.009$ [27], which are in agreement with our estimates, within the error bars (cf. Tab. 3). It should be mentioned that all exponents obtained, for both critical frontiers of the DKCA, fall in the universality class of DP (precise estimates of the exponents of DP are included in Tab. 3 for completeness).

To conclude, we have investigated the Domany-Kinzel cellular automaton using two different numerical approaches, namely, the spontaneous-search method and the short-time-dynamics technique. We have shown that the spontaneous-search method is adequate for estimating precisely the critical borders of the automaton, i.e., the frozen-active, as well as the nonchaotic-chaotic critical frontiers. In addition to that, this method produced accurate estimates for the critical exponent $\nu_\perp$ on both critical frontiers investigated. Using the critical frontiers obtained, we have applied the short-time-dynamics approach in order to find other critical exponents. To our knowledge, such a technique was never applied in an investigation of the critical frontier nonchaotic-chaotic of

the Domany-Kinzel cellular automaton. All exponents obtained, for both critical frontiers studied, fall in the universality class of directed percolation. The present analysis provides further reliability to both techniques, and in particular, to the spontaneous-search method, which has been already applied successfully in the study of the critical properties of polymers [14], percolation [15], as well as of magnetic systems [16–18], and may be implemented in the future also for investigating other systems exhibiting critical behavior.

The partial financial supports from CNPq, Pronex/FAPERJ, and FAPEPI (Brazilian agencies) are acknowledged.

References

1. S. Wolfram, *Theory and Applications of Cellular Automata* (World Scientific, Singapore, 1986)
2. J. Marro, R. Dickman, *Nonequilibrium Phase Transitions in Lattice Models* (Cambridge University Press, Cambridge, 1999)
3. H. Hinrichsen, Adv. Phys. **49**, 815 (2000)
4. E. Domany, W. Kinzel, Phys. Rev. Lett. **53**, 311 (1984)
5. W. Kinzel, Z. Phys. B **58**, 229 (1985)
6. M.L. Martins, H.F. Verona de Resende, C. Tsallis, A.C.N. de Magalhães, Phys. Rev. Lett. **66**, 2045 (1991)
7. H.K. Jansen, Z. Phys. B **42**, 151 (1981)
8. P. Grassberger, Z. Phys. B **47**, 365 (1982)
9. J.W. Essam, J. Phys. A **22**, 4927 (1989)
10. R. Dickman, A.Y. Tretyakov, Phys. Rev. E **52**, 3218 (1995)
11. P. Grassberger, J. Stat. Phys. **79**, 13 (1995)
12. P. Bak, C. Tang, K. Wiesenfeld, Phys. Rev. A **38**, 364 (1988)
13. D. Sornette, A. Johansen, I. Dornic, J. Phys. I France **5**, 325 (1995)
14. J.S. Andrade Jr., L.S. Lucena, A.M. Alencar, J.E. Freitas, Physica A **238**, 163 (1997)
15. A.M. Alencar, J.S. Andrade Jr., L.S. Lucena, Phys. Rev. E **56**, R2379 (1997)
16. U.L. Fulco, L.S. Lucena, G.M. Viswanathan, Physica A **264**, 171 (1999)
17. U.L. Fulco, F.D. Nobre, L.R. da Silva, L.S. Lucena, G.M. Viswanathan, Physica A **284**, 223 (2000)
18. U.L. Fulco, F.D. Nobre, L.R. da Silva, L.S. Lucena, Physica A **297**, 131 (2001)
19. B. Zheng, Int. J. Mod. B **12**, 1419 (1998)
20. H.K. Janssen, B. Schaub, B. Schmittmann, Z. Phys. B **73**, 539 (1989)
21. Z.B. Li, L. Schulke, B. Zheng, Phys. Rev. E **53**, 2940 (1996)
22. P. Grassberger, Y. Zhang, Physica A **224**, 169 (1996)
23. T. Tomé, M.J. de Oliveira, Phys. Rev. E **58**, 4242 (1998)
24. R. da Silva, N.A. Alves, J.R. Drugowich de Felicio, Phys. Rev. E **66**, 026130 (2002)
25. T.F. Nagy, S.D. Mahanti, C. Tsallis, Physica A **250**, 345 (1998)
26. A.P.F. Atman, R. Dickman, J.G. Moreira, Phys. Rev. E **66**, 016113 (2002)
27. R. da Silva, R. Dickman, J.R.D. de Felicio, Phys. Rev. E **70**, 067701 (2004)
28. W. Kinzel, in *Ann. Isr. Phys. Soc.* edited by G. Deutscher, R. Zallen, J. Adler (Adam Hilger, Bristol, 1983) Vol. 5
29. I. Jensen, J. Phys. A **32**, 5233 (1999)